JOURNAL OF SPACECRAFT AND ROCKETS
Vol. 37, No. 1, January–February 2000

Aerogravity-Assist Trajectories to the Outer Planets and the Effect of Drag

Jon A. Sims*
Jet Propulsion Laboratory, California Institute of Technology, Pasadena, California 91109-8099
James M. Longuski†
Purdue University, West Lafayette, Indiana 47907-1282
and
Moonish R. Patel‡
Lockheed Martin Missiles and Space Company, Sunnyvale, California 94089

Automated trajectory design software is used to thoroughly search the near-future trajectory space for missions with low launch energies to the outer planets using aerogravity assists at Venus and Mars and at Mars alone. Aerogravity assist is shown to reduce the required hyperbolic excess launch velocities and total flight times by more than half for these missions. An analytic approach is validated using results from the automated search and then is augmented to account for drag losses during the aerogravity-assist maneuvers. The effect that the drag loss has on the interplanetary trajectories is examined. Drag increases the minimum launch energy required to reach a particular planet and increases the flight time for those trajectories that do reach a planet; however, the increase is small compared to the overall reductions achieved using aerogravity assist. Calculations including drag indicate that an aerogravity-assisted spacecraft using lift-to-drag ratios of 10 at Venus and 5 at Mars can reach Pluto with a hyperbolic excess launch velocity of only 7 km/s and a time of flight of only seven years.

Nomenclature

C_3 = V_∞^2, km^2/s^2
D = drag, N
g_{aero} = aerodynamic g-load, g
L = lift, N
m = spacecraft mass, kg
r = radius, km
t = time
$\boldsymbol{V}$ = spacecraft velocity, km/s
$\boldsymbol{V}_P$ = planet velocity, km/s
$\boldsymbol{V}_\infty$ = hyperbolic excess velocity, km/s
δ = gravitational turn angle, deg
θ = aerodynamic turn angle, deg
μ = gravitational parameter, km^3/s^2
ϕ = total turn angle (gravitational plus aerodynamic), deg

Subscripts

p = periapsis
1 = before aerodynamic turn
2 = after aerodynamic turn

Superscripts

$-$ = before a flyby
$+$ = after a flyby

Introduction

GRAVITY assist is a proven technique in interplanetary exploration, as exemplified by the missions of the Voyager and Galileo spacecraft. The technique can be used to reduce the launch energy requirements and flight time for a given mission or to increase the science return by enabling more planetary, satellite, or asteroid encounters. The gravity-assist technique is limited, however, by the turn angle (of the $\boldsymbol{V}_\infty$ vector) that can be effected by a flyby body. This turn angle depends on the size and mass of the planet and the $\boldsymbol{V}_\infty$. One method of circumventing this turn angle limitation is to use aerogravity assist. In this method, a lifting body flies through the atmosphere of the planet to turn the $\boldsymbol{V}_\infty$ in any desired direction.

A typical aerogravity-assist trajectory relative to a flyby body is shown in Fig. 1. The spacecraft approaches the body on a hyperbolic orbit. After reaching periapsis within the upper atmosphere of the body, the spacecraft flies at a nearly constant radius with aerodynamic lift directed downward. When the appropriate amount of turn has been achieved, the spacecraft exits the atmosphere and continues along a hyperbolic orbit.

The flight within the atmosphere allows the $\boldsymbol{V}_\infty$ to be turned in any desired direction; however, the drag on the spacecraft continuously reduces the speed with the result that V_∞^+ is less than V_∞^- (in fact, the turn angle may be limited to ensure V_∞^+ remains positive). The higher the lift-to-drag ratio (L/D), the lower the reduction in $\boldsymbol{V}_\infty$ due to drag will be.

One type of vehicle that can achieve high lift-to-drag ratios at hypersonic speeds is a waverider. A waverider is designed so that the shock wave remains attached to the leading edge, giving the appearance that the vehicle is riding on top of the shock wave. The high lift is generated by the high pressure behind the shock wave under the vehicle. The idea for such a vehicle was introduced by Nonweiler.[1] Spurred by the high interest in hypersonic flight in recent years, significant research activity[2,3] has been devoted to optimizing waverider shapes to obtain high L/D. Lift-to-drag ratios as high as 15 in the atmosphere of Venus have been calculated for some optimized hypersonic waverider configurations.[4] Anderson[5] considers hypersonic waveriders to be a "breakthrough technology option," potentially supporting solar system missions in the near future.

Previous investigators have demonstrated the advantages of using aerogravity assist for interplanetary missions. The major advantages are low launch $\boldsymbol{V}_\infty$and very short flight times. Bender[6] analyzes aerogravity assists using Venus and Mars. Ignoring drag losses, he selects certain trajectory types between Earth, Venus, and

Received 23 November 1998; revision received 1 August 1999; accepted for publication 1 August 1999.

*Member of Engineering Staff, Navigation and Flight Mechanics Section, Mail Stop 301-142, 4800 Oak Grove Drive. Senior Member AIAA.
†Professor, School of Aeronautics and Astronautics. Associate Fellow AIAA.
‡Senior Systems Engineer, Organization K2-46, Building 150, 1111 Lockheed Martin Way. Member AIAA.

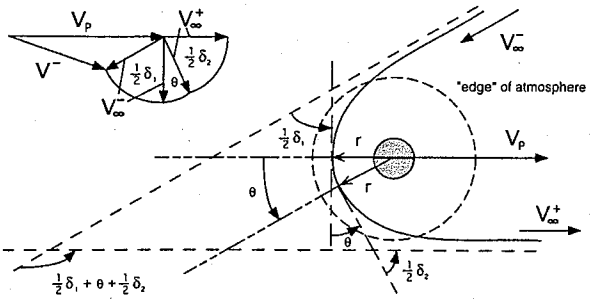

Fig. 1 Aerogravity assist.

Mars and determines the planetary phasing and flyby conditions for trajectories with low launch energy at Earth ($C_3 \leq 30$ km^2/s^2) to reach the outer planets (Saturn and beyond). Once approximate launch dates are determined from this analysis, he uses an optimization program to find a total of nine trajectories (three to Saturn, three to Uranus, two to Neptune, and one to Pluto). McRonald and Randolph[7] consider using Venus and Mars aerogravity assists for missions to the sun and to Pluto. They demonstrate that less launch energy is required to achieve a desired heliocentric energy using Venus and Mars than using Mars alone, which requires less than using Venus alone. Assuming circular, coplanar orbits and ignoring phasing constraints and drag losses, McRonald and Randolph discuss the characteristics of trajectories using Venus and/or Mars aerogravity assists. They also present two trajectories to the sun, one using Venus and Mars and another using Mars only. In another paper, Randolph and McRonald[8] discuss parametric studies of launch opportunities for missions to Uranus, Neptune, and Pluto using aerogravity assists at Venus and Mars. These studies assume circular, coplanar orbits and restrict the trajectory types from Earth to Venus and Venus to Mars. Randolph and McRonald mention drag loss but essentially ignore it when determining launch opportunities. They state that the present technology for computation of heating in the atmosphere is bounded by speeds of about 15 km/s at Earth, Venus, and Mars. Trying to remain within this bound, they limit the launch V_∞ to 6.6 km/s or less. In addition to these parametric studies, three trajectories are presented: one each to the sun, Saturn, and Pluto, all of which use aerogravity assists at Venus and Mars. Unfortunately, the atmospheric speeds of these trajectories exceed 15 km/s at Mars.

In general, these authors[6–8] predict approximate launch dates for some representative trajectories to the outer planets using aerogravity assists at Venus and/or Mars; however, they overlook some opportunities due to their assumptions of certain trajectory types. Furthermore, drag losses are ignored in all of the trajectories presented in these papers.[6–8] Although the possible effect on the interplanetary trajectories of drag losses during the aerogravity-assist maneuvers is sometimes mentioned, no detailed analysis is given.

In this paper we extend the previous analysis in two major aspects. First, we perform a thorough analysis of the trajectory space for low launch energy trajectories to the outer planets with aerogravity assists at Venus and Mars in succession and at Mars alone. Lower launch energies not only allow the use of larger spacecraft (enhanced scientific return) or smaller launch vehicles (reduced cost), but for aerogravity assists they also minimize atmospheric velocity and, therefore, the heating and aerodynamic g-load. Second, we develop an analytic approach for an initial assessment of the drag loss effect.

In this study we use an automated version of the Satellite Tour Design Program (STOUR).[9,10] STOUR is ordinarily used for the design of patched-conic gravity-assist trajectories, but with the appropriate input we can use it to find aerogravity-assist trajectories. The program uses C_3 (or V_∞) matching at an encounter to find potential trajectories to the next target. For each trajectory with the correct V_∞, the program determines the required turn angle and corresponding flyby radius at the encounter. The trajectories with a flyby radius greater than the prescribed minimum are kept, whereas all others are discarded. An aerogravity assist has an unrestricted turn angle. To simulate this in STOUR, we allow the flyby radius to take on any value, even below the surface of the planet. For a gravity assist that requires a negative flyby altitude, the aerodynamic turn angle provided by the flight through the atmosphere will make up for the reduction in gravity turn angle as the flyby altitude is moved to a positive value. In STOUR, the incoming V_∞ equals the outgoing V_∞ at an encounter, so that the energy loss due to drag is not taken into account. (This is the hypothetical case in which L/D is effectively infinity.) The analytic approach allows us to correct for the drag loss.

Aerogravity-Assist Trajectories Using Venus and Mars

As a first step in characterizing trajectories to the outer planets using aerogravity assists at Venus and Mars, we consider the Earth–Venus–Mars leg of these trajectories. The flyby of Venus may or may not require an aerogravity assist. The trajectory families occur about every 1.6 years, the synodic period between Earth and Venus. Within each family are groups of trajectories corresponding to different trajectory types. We allow up to two complete orbits of the spacecraft (about the sun) between Earth and Venus and between Venus and Mars (see Ref. 11 for details), a larger range than considered by Bender[6] or Randolph and McRonald.[8] Previously, more than one complete orbit between Venus and Mars was thought to require too long a flight time, but we will show that some relatively fast trajectories to the outer planets include more than one complete orbit about the sun.

Figure 2 shows Earth–Venus–Mars trajectories to Saturn. We consider launch dates from the year 2000 through 2015 with a 15-day step size. We searched for trajectories with launch hyperbolic excess velocities ranging from 3.0 to 7.0 km/s in steps of 0.5 km/s but plotted the results for only 4.5 and 5.5 km/s (with flight times up to 5.5 years) for clarity. We chose these relatively low launch energies for the reasons described earlier. Additional characteristics of eight representative trajectories with launch hyperbolic excess velocities up to 5.5 km/s are presented in Table 1. The aerodynamic turn angle in Table 1 is computed in the following manner. We use the flyby altitude (potentially subsurface) output by STOUR to determine the total turn angle that is required using the following well-known relation for hyperbolic orbits:

$$\sin(\delta/2) = 1/\left(1 + r_p V_\infty^2/\mu\right) \tag{1}$$

We then calculate the gravity turn angle based on a periapsis altitude of 100 km at Venus and 60 km at Mars. The aerodynamic turn angle is the difference between the total turn angle and the gravity turn angle. The aerodynamic g-load is the lift force per unit mass required to keep the spacecraft on a circular trajectory (constant radius) through the atmosphere. (The g-load is given in the standard gravitational acceleration on the Earth, g.) The normal component of acceleration for a circular trajectory at the periapsis radius is V_p^2/r_p. The gravitational acceleration at this radius is μ/r_p^2. Because the lift and gravity both act in the normal direction, we have

$$g_{\text{aero}} = V_p^2/r_p - \mu/r_p^2 \tag{2}$$

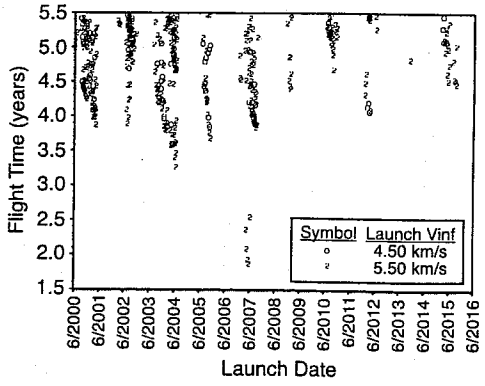

Fig. 2 Earth–Venus–Mars–Saturn opportunities.

Table 1 Sample Venus–Mars aerogravity-assist trajectories to Saturn

Parameter	Launch date, C_3, $(km/s)^2$							
	27 Sept. 2003, 20.25	11 Nov. 2003, 16.00	9 May 2004, 16.00	9 May 2004, 20.25	8 July 2004, 30.25	9 May 2007, 25.00	8 June 2007, 25.00	23 June 2007, 30.25
Venus flyby								
Time, days	409	380	175	183	151	107	80	69
V_∞, km/s	6.76	6.54	8.33	9.16	10.97	9.79	10.65	10.25
θ, deg	0	0	79.2	91.9	34.8	57.1	70.0	80.6
Flyby alt., km	6564	1520	AGA[a]	AGA	AGA	AGA	AGA	AGA
g_{aero}, g	0	0	2.02	2.27	2.87	2.46	2.75	2.61
Mars flyby								
Time, days	722	708	499	529	438	207	172	168
V_∞, km/s	9.47	10.20	10.01	10.97	10.73	13.86	15.30	12.99
θ, deg	89.2	110.6	89.5	109.2	90.9	67.9	75.4	60.2
g_{aero}, g	3.01	3.43	3.32	3.91	3.76	6.03	7.27	5.34
Saturn arrival								
Time								
Days	1738	1562	1441	1316	1319	887	776	931
Years	4.76	4.28	3.95	3.60	3.61	2.43	2.12	2.55
Date	30 June 2008	20 Feb. 2008	19 April 2008	16 Dec. 2007	17 Feb. 2008	12 Oct. 2009	23 July 2009	9 Jan. 2010
V_∞, km/s	11.65	14.45	12.98	16.14	14.29	19.24	22.39	16.45

[a]Required aerogravity assist.

Table 2 Sample Venus–Mars aerogravity-assist trajectories to Pluto

Parameter	Launch date, C_3, $(km/s)^2$							
	25 Feb. 2004, 25.00	11 March 2004, 20.25	14 March 2012, 16.00	4 Sept. 2013, 49.00	4 Oct. 2013, 36.00	3 Nov. 2013, 49.00	27 May 2015, 49.00	26 June 2015, 49.00
Venus flyby								
Time, days	110	99	99	115	95	64	147	131
V_∞, km/s	9.82	9.65	8.61	12.01	11.69	14.45	10.97	10.51
θ, deg	24.3	27.9	20.5	57.3	86.6	94.4	40.3	31.0
g_{aero}, g	2.47	2.42	2.10	3.26	3.14	4.33	2.87	2.71
Mars flyby								
Time, days	854	848	663	209	188	143	256	233
V_∞, km/s	14.27	14.14	11.90	21.73	19.80	25.39	18.78	17.75
θ, deg	97.1	105.3	90.1	67.5	56.1	76.7	76.9	67.2
g_{aero}, g	6.37	6.26	4.54	14.29	11.92	19.37	10.76	9.65
Pluto arrival								
Time								
Days	3814	3893	5321	2144	2522	1746	2500	2763
Years	10.44	10.66	14.57	5.87	6.90	4.78	6.84	7.56
Date	5 Aug. 2014	7 Nov. 2014	8 Oct. 2026	19 July 2019	30 Aug. 2020	15 Aug. 2018	31 March 2022	18 Jan. 2023
V_∞, km/s	16.29	15.72	10.09	27.47	22.26	33.72	23.80	20.77

Two of the trajectories in Table 1 have positive flyby altitudes at Venus, and so they do not need to enter the atmosphere at Venus. This situation can be desirable because the current approach is to optimize the shape of a waverider for specific flight conditions.[4] The performance, L/D, may be compromised for a spacecraft that must fly through the atmospheres of both Venus and Mars, although the flight conditions may be similar enough that the performance degradation is not substantial.

The trajectory in Table 1 with a launch date of 11 November 2003 has several desirable characteristics: low launch V_∞ (4.0 km/s), no atmospheric passage at Venus (flyby altitude, 1520 km), and relatively short time of flight (4.28 years). The speed in the atmosphere during the Mars aerogravity assist is 11.3 km/s (resulting from the V_∞ of 10.2 km/s), well within present technology for computing the aerodynamic heating properties as described earlier ($\leq$15 km/s).

Figure 3 shows Earth–Venus–Mars trajectories to Pluto, and more details of eight trajectories are presented in Table 2. For the trajectories to Pluto, we searched over the same range of launch hyperbolic excess velocities as we did for the trajectories to Saturn, but here we plotted the results for 5.0 and 7.0 km/s and presented results in Table 2 for launch hyperbolic excess velocities up to 7.0 km/s. We did this to show that the time of flight can be significantly reduced with a slightly higher launch V_∞, but at a cost of higher atmospheric speeds.

Plots analogous to Figs. 2 and 3 for Earth–Venus–Mars trajectories to Jupiter, Uranus, and Neptune (individually), along with additional characteristics of sample trajectories, are provided by Sims et al.[11] In addition to the handful of trajectories presented in the literature, we have found literally hundreds of opportunities. The trajectories presented in Tables 1 and 2 and in Ref. 11 are representative of the possibilities. They have not been optimized. Even so, they demonstrate the ability of aerogravity-assist trajectories to reach the outer planets with relatively short flight times and low launch energies. We can use optimization programs to finely

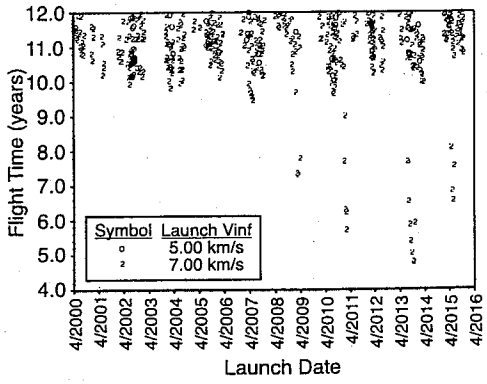

Fig. 3 Earth–Venus–Mars–Pluto opportunities.

Table 3 Sample Mars aerogravity-assist trajectories to Saturn

	Launch date, C_3, $(km/s)^2$							
Parameter	20 March 2001, 20.25	8 June 2003, 25.00	8 June 2003, 30.25	23 June 2003, 42.25	23 June 2003, 64.00	8 July 2003, 56.25	11 Aug. 2005, 56.25	11 Aug. 2005, 64.00
				Mars flyby				
Time, days	120	105	98	80	70	70	99	95
V_∞, km/s	10.09	8.32	9.29	10.66	13.04	10.87	10.77	11.51
θ, deg	132.7	88.9	99.1	105.3	115.6	104.2	41.6	50.9
g_{aero}, g	3.37	2.41	2.91	3.72	5.38	3.85	3.79	4.27
				Saturn arrival				
Time								
Days	1550	1209	1079	941	830	896	1000	872
Years	4.24	3.31	2.95	2.58	2.27	2.45	2.74	2.39
Date	17 June 2005	29 Sept. 2006	22 May 2006	19 Jan. 2006	30 Sept. 2005	20 Dec. 2005	7 May 2008	31 Dec. 2007
V_∞, km/s	7.27	10.09	12.10	14.62	17.53	15.41	12.96	15.92

Table 4 Sample Mars aerogravity-assist trajectories to Pluto

	Launch date, C_3, $(km/s)^2$							
Parameter	25 May 1997, 64.00	30 May1999, 64.00	18 Nov. 2009, 56.25	18 Nov. 2009, 64.00	23 Nov. 2011, 64.00	8 Dec. 2011, 49.00	8.Dec. 2011, 56.25	8 Dec. 2011, 64.00
				Mars flyby				
Time, days	1221	1176	111	106	128	122	117	113
V_∞, km/s	14.24	14.01	12.76	13.68	14.29	13.64	14.45	15.23
θ, deg	77.2	74.1	98.0	103.7	66.1	51.5	62.1	69.6
g_{aero}, g	6.34	6.15	5.17	5.88	6.39	5.85	6.52	7.20
				Pluto arrival				
Time								
Days	4252	4297	3984	3654	3292	4116	3286	2930
Years	11.64	11.76	10.91	10.00	9.01	11.27	9.00	8.02
Date	14 Jan. 2009	5 March 2011	15 Oct. 2020	20 Nov. 2019	27 Nov. 2020	16 March 2023	6 Dec. 2020	16 Dec. 2019
V_∞, km/s	15.31	14.97	12.25	13.64	15.68	11.84	15.64	17.95

tune trajectories found by STOUR to improve specific characteristics.

Aerogravity-Assist Trajectories Using Mars Alone

The trajectories in the preceding section included flybys of Venus and Mars with an aerogravity assist at both in most cases. Waveriders having the highest L/D are optimized for specific flight conditions, and so we also want to analyze trajectories that include only one possible aerogravity assist. Using Venus alone to reach the outer planets requires hyperbolic excess velocities at Venus that result in atmospheric speeds above 15 km/s. The minimum V_∞ at Venus to reach Jupiter is 11.4 km/s, corresponding to an atmospheric speed of 15.3 km/s. The hyperbolic excess velocities at Mars to reach the outer planets are much less. For example, to reach Neptune requires a V_∞ at Mars of 9.2 km/s with a corresponding atmospheric speed of 10.4 km/s.

For aerogravity-assist trajectories using Mars alone, we increase the search range to include higher Earth launch energies. We can increase the search range while still maintaining low atmospheric speeds for two reasons: a given Earth launch V_∞ results in a lower V_∞ at Mars than at Venus, and a given V_∞ at Mars results in a lower atmospheric speed than the same V_∞ would at Venus. We also begin the search with earlier launch dates because, in some cases, relatively short time-of-flight trajectories occur late in this decade and do not appear again for more than 15 years.

Earth–Mars trajectories to Saturn and Pluto are shown in Figs. 4 and 5, respectively. Analogous plots for trajectories to Jupiter, Uranus, and Neptune are provided by Sims et al.[11] The effect of the synodic period between Earth and Mars (2.1 years) is readily apparent for different trajectory types. The longer period phenomenon (on the order of decades) is a result of the relative alignment between Mars and the destination outer planet, in addition to the Earth–Mars relative alignment. Sample trajectories are presented in Tables 3 and 4 and in Ref. 11. In general, for a given time of flight to an outer planet, an Earth–Venus–Mars trajectory will require less launch V_∞, but an Earth–Mars trajectory will have a lower V_∞ at Mars.

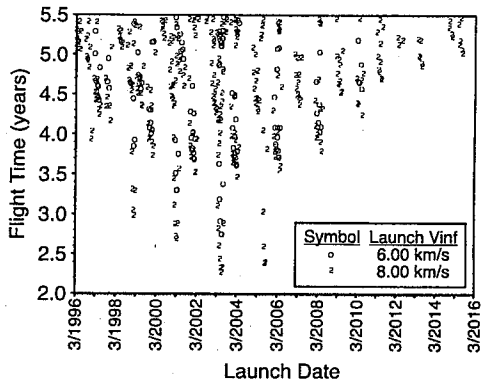

Fig. 4 Earth–Mars–Saturn opportunities.

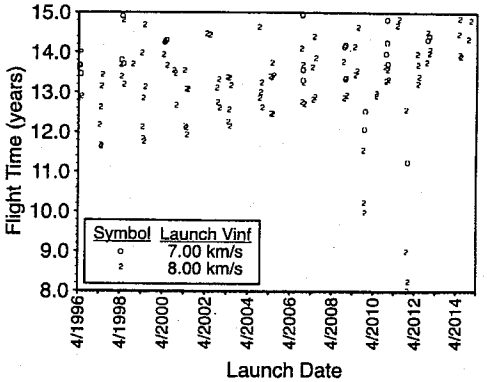

Fig. 5 Earth–Mars–Pluto opportunities.

Table 5 Shortest times of flight for Venus–Mars aerogravity-assist trajectories to the outer planets (STOUR/analytic, years)

Launch V_∞, km/s	Destination planet				
	Jupiter	Saturn	Uranus	Neptune	Pluto
3.5	2.68/1.80	6.58/3.23	7.83/7.28	No trajectory[a]/12.92	No trajectory[a]/——
4.0	2.33/1.45	3.94/2.41	5.36/4.71	8.94/7.46	14.57/8.86
4.5	2.18/1.29	3.59/2.08	4.66/3.95	7.50/6.12	10.66/6.64
5.0	2.09/1.18	2.12/1.89	4.28/3.53	6.78/5.42	10.02/6.11
5.5	2.04/1.10	1.88/1.76	4.11/3.25	5.77/4.96	9.92/5.58
6.0	2.01/1.05	1.77/1.66	3.64/3.04	5.02/4.63	6.27/5.18
6.5	1.42/1.00	1.70/1.57	3.30/2.88	4.42/4.37	5.23/4.86
7.0	1.26/0.96	1.65/1.51	3.17/2.75	4.25/4.16	4.78/4.61

[a]STOUR found no trajectories with time of flight <15 years.

Analytic Investigation: No Drag

Our next step is to analyze the effect that the drag losses during the planetary flybys have on the interplanetary trajectories. In principle, one could specify a spacecraft and, using detailed models of the planetary atmospheres and the significant forces, numerically integrate the entire trajectory from launch to final planet. This type of analysis is beyond the scope of this paper, however, and represents a difficult problem that has not been addressed in the literature. Instead, we develop a measure of merit for the trajectories to complement a simplified model. We first determine how well this model and measure of merit (shortest time of flight) describe the trajectories presented earlier that do not include drag; we then augment our model to include drag and analyze the resulting trajectories.

We consider circular, coplanar orbits for the planets and determine the time of flight from launch to the destination planet, assuming that each flyby (at Venus and Mars) places the spacecraft at perihelion of the resulting orbit. In reference to Fig. 1, we align $\boldsymbol{V}_\infty^+$ with $\boldsymbol{V}_p$. We also assume that the first time the spacecraft crosses the orbit of the next flyby planet the planet is conveniently located there; that is, there are no phasing constraints. This analysis produces a time of flight that is very close to the minimum possible for a given flyby sequence and launch energy. These analytic times of flight along with the shortest times of flight from the STOUR runs (15-day time steps with launch dates in 2000–2015) are provided in Table 5. (Because of the large eccentricity of Pluto's orbit, the analytic times of flight were calculated using the actual orbital radius of Pluto when the corresponding STOUR trajectory arrives.) We note that none of the flight times from STOUR are shorter than the analytic minimum flight times. In many cases the flight times are relatively close, indicating the actual planetary alignments are close to ideal. For example, STOUR found a trajectory that took 1.77 years to reach Saturn with a launch V_∞ of 6.0 km/s; if the planets were aligned such that each flyby placed the spacecraft at perihelion, the analytic flight time to Saturn is 1.66 years for the same launch V_∞. In other cases, the minimum flight time from STOUR is significantly larger than the analytic minimum, indicating that the four planets (Earth, Venus, Mars, and destination outer planet) did not align ideally during the 16-years span of launch dates. It is expected that reducing the time step in STOUR and increasing the launch date range would result in trajectories with flight times closer to the predicted minimum flight times. None of the STOUR trajectories had flight times shorter than our analytic minimums, but many were close. Therefore, the analytic theory provides a good bound on the flight time.

The launch hyperbolic excess velocities for a Hohmann-type transfer directly from Earth to each of the outer planets, and the corresponding times of flight, are presented in Table 6. The minimum launch V_∞ and time of flight for a trajectory from Earth to Pluto are similar to those to Neptune for the early part of the 21st century, because Pluto's orbit has a relatively large eccentricity and recently passed through perihelion (1990). A single Mars gravity assist without flying through the atmosphere can reduce the launch hyperbolic excess velocities in Table 6 by less than 1 km/s. Also, without flying through the atmosphere, a single Venus gravity assist or a Venus gravity assist followed by a Mars gravity assist has worse performance to the outer planets than the direct ballistic transfers. We also note that for all of the trajectories presented in Figs. 2–5 at least one of the flybys is an aerogravity assist; none of the trajectories are strictly gravity assist. Hence, the dramatic advantages of aerogravity assist are clear: very short flight times with low launch energies.

Table 6 Hohmann-type transfer

Destination planet	Launch V_∞, km/s	Time of flight, yr
Jupiter	8.8	2.7
Saturn	10.3	6.0
Uranus	11.3	16
Neptune	11.7	31

Analytic Investigation: Drag

We now will incorporate drag into our analytic model and determine how it affects the measure of merit, flight time to the outer planets. In Eq. (2), we considered the forces and acceleration in the direction normal to the flight path to determine the aerodynamic g-load. For a circular flight path, drag acts in the tangential direction. The component of Newton's second law, $\boldsymbol{F} = m\boldsymbol{a}$, in the tangential direction can be written

$$-D = m\frac{\mathrm{d}V}{\mathrm{d}t} \tag{3}$$

where D is the magnitude of the drag force acting in the direction opposite to the velocity. Because the performance of a vehicle is often characterized by L/D, we rearrange Eq. (3) as follows:

$$\mathrm{d}V = -\frac{(L/D)}{(L/D)}\frac{D}{m}\mathrm{d}t = -\frac{1}{(L/D)}\frac{L}{m}\mathrm{d}t \tag{4}$$

Recalling the aerodynamic turn angle in Fig. 1, we can write

$$\mathrm{d}t = (r/V)\,\mathrm{d}\theta \tag{5}$$

where r is the radius of the circular trajectory. The aerodynamic g-load is the lift force per unit mass, L/m. Substituting Eqs. (5) and (2) (in this context V_p is V and r_p is r) into Eq. (4), we obtain

$$\mathrm{d}V = -\frac{1}{(L/D)}\left(\frac{V^2}{r} - \frac{\mu}{r^2}\right)\frac{r}{V}\mathrm{d}\theta \tag{6}$$

To determine the decrease in velocity during this segment of the flight, we rearrange Eq. (6) and integrate from $V = V_1$ at $\theta = \theta_1 = 0$ to $V = V_2$ at $\theta = \theta_2 = \theta$:

$$\int_0^\theta \mathrm{d}\theta = -\int_{V_1}^{V_2}\left(\frac{L}{D}\right)\frac{1}{V - (\mu/rV)}\mathrm{d}V \tag{7}$$

We will assume that L/D is constant, a good approximation as long as the velocity remains higher than the local circular velocity, $\sqrt{(\mu/r)}$. In this case Eq. (7) can be written

$$\int_0^\theta \mathrm{d}\theta = -\left(\frac{L}{D}\right)\int_{V_1}^{V_2}\frac{V}{V^2 - \mu/r}\mathrm{d}V \tag{8}$$

Let

$$x = V^2 - \mu/r \tag{9}$$

Then, assuming r is constant,

$$\mathrm{d}x = 2V\,\mathrm{d}V \tag{10}$$

Substituting Eqs. (9) and (10) into Eq. (8), we obtain

$$\int_0^{\theta} \mathrm{d}\theta = -\left(\frac{L}{D}\right)\frac{1}{2}\int_{x_1}^{x_2}\frac{\mathrm{d}x}{x} \tag{11}$$

and so

$$\theta|_0^{\theta} = -\tfrac{1}{2}(L/D)\,\ell n(x)|_{x_1}^{x_2} \tag{12}$$

Hence, recalling Eq. (9), we have

$$\theta = -\frac{1}{2}\left(\frac{L}{D}\right)\ell n\left[\frac{V_2^2 - \mu/r}{V_1^2 - \mu/r}\right] \tag{13}$$

We can solve Eq. (13) for V_2 in terms of V_1 and θ. Rewriting Eq. (13) in the form

$$\exp\left[\frac{-2\theta}{(L/D)}\right] = \frac{V_2^2 - \mu/r}{V_1^2 - \mu/r} \tag{14}$$

and solving for V_2, we have

$$V_2 = \sqrt{\exp[-2\theta/(L/D)]V_1^2 - \{\exp[-2\theta/(L/D)] - 1\}(\mu/r)} \tag{15}$$

For interplanetary mission design, we want to know the effect on V_∞. For the incoming and outgoing hyperbolic orbits, we can write

$$V_1^2 = 2\mu/r + V_\infty^{-2}, \qquad V_2^2 = 2\mu/r + V_\infty^{+2} \tag{16}$$

In writing Eqs. (16), we have disregarded the velocity loss on the portions of the trajectory leading to and departing from the circular flight. Substituting these equations into Eq. (15), we obtain (after some algebra)

$$V_\infty^{+} = \sqrt{\exp[-2\theta/(L/D)]V_\infty^{-2} + \{\exp[-2\theta/(L/D)] - 1\}(\mu/r)} \tag{17}$$

Equation (17), also presented by Anderson et al.,[4] is an expression for the outgoing hyperbolic excess velocity as a function of the aerodynamic turn angle. A plot of this relationship at Venus with $r = 6152$ km (altitude = 100 km) and $V_\infty^- = 10$ km/s is presented in Fig. 6.

Because V_∞^+ is less than V_∞^-, the gravitational turn angle after the atmospheric flight, $\delta_2/2$, is greater than before the atmospheric flight, $\delta_1/2$. We can derive an expression for $\delta_2/2$ in terms of V_∞^- and θ. From Eq. (1)

$$\sin(\delta_2/2) = 1\Big/\left(1 + rV_\infty^{+2}/\mu\right) \tag{18}$$

Equation (17) can be rearranged to obtain

$$1 + rV_\infty^{+2}/\mu = \exp[-2\theta/(L/D)]\left\{rV_\infty^{-2}/\mu + 1\right\} \tag{19}$$

Substituting Eq. (19) into Eq. (18), we find

$$\sin\left(\frac{\delta_2}{2}\right) = \frac{\exp[2\theta/(L/D)]}{1 + rV_\infty^{-2}/\mu} \tag{20}$$

Using

$$\sin(\delta_1/2) = 1\Big/\left(1 + rV_\infty^{-2}/\mu\right) \tag{21}$$

we note that Eq. (20) becomes

$$\sin(\delta_2/2) = \exp[2\theta/(L/D)]\sin(\delta_1/2) \tag{22}$$

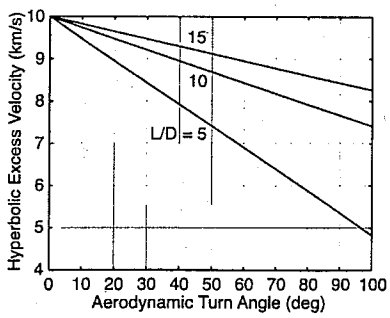

Fig. 6 Reduction in V_∞ due to drag.

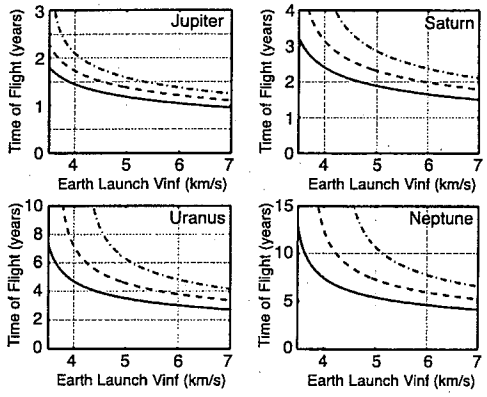

Fig. 7 Earth–Venus–Mars–outer planet trajectories including drag (——, no drag; – – –, L/D is 15 at Venus and 10 at Mars; and – · –, L/D is 10 at Venus and 5 at Mars).

The total turn angle ϕ is given by

$$\phi = \delta_1/2 + \theta + \delta_2/2 \tag{23}$$

Using Eqs. (20) and (21), we can write Eq. (23) in the form

$$\phi = \sin^{-1}\left[\frac{1}{1 + rV_\infty^{-2}/\mu}\right] + \theta + \sin^{-1}\left\{\frac{\exp[2\theta/(L/D)]}{1 + rV_\infty^{-2}/\mu}\right\} \tag{24}$$

Equation (24) has also been presented by Lewis.[12]

We now determine the effect drag losses have on the interplanetary trajectories by incorporating Eq. (17) into our analytic model. As in the preceding section, we assume that each flyby places the spacecraft at perihelion of the resulting orbit. This procedure overestimates the minimum time of flight: the turn angle is larger than it should be (for minimum flight time) even without drag, and the larger turn angle leads to a smaller V_∞^+. Furthermore, we approximate the total gravitational turn angle as twice the smaller initial value, $\delta_1/2$. Hence, we overestimate the required aerodynamic turn angle. The resulting flight times to the outer planets are shown in Fig. 7 for three cases: 1) L/D of 10 at Venus and 5 at Mars, 2) L/D of 15 at Venus and 10 at Mars, and 3) the hypothetical case of no drag (L/D of ∞). At low launch energies, the flight time is sensitive to the value of L/D, and the drag losses significantly increase the flight time. From another point of view, the minimum launch V_∞ to reach a planet is higher. However, for slightly higher launch energies, the increase in flight time is not large when compared to the savings in flight time using aerogravity assist, and the sensitivity to the value of L/D is much smaller.

Several methods can be used to offset or minimize the drag effects. One way is to reduce the drag, for example, by using waveriders with high L/D. Another way is to compensate for the velocity loss by adding velocity 1) before, 2) during, or 3) after the aerogravity-assist maneuver, as follows.

1) Increase the launch energy. The increase in launch energy will change the character of the trajectory and increase the heating during

the atmospheric flight; however, the spacecraft itself does not have to carry as much propellant.

2) Thrust during the atmospheric flight. Thrusting will help to maintain the optimum conditions for waverider performance. One practical method to partially offset the drag during the atmospheric flight is to expel the working fluid of an active cooling system.[13]

3) Include a propulsive maneuver after the aerogravity-assist maneuver.

We have examined the drag loss effect analytically using a simplified model. A natural extension to this work is to incorporate Eq. (17) into STOUR, the automated trajectory design software. We leave this for future work.

Conclusion

The trajectory space to the outer planets using aerogravity assists at Venus and Mars and at Mars without Venus has been mapped out for low launch energies and a wide range of launch dates. Aerogravity assists significantly reduce the required launch energies and times of flight to the outer planets.

An analytic approach shows that for high lift-to-drag vehicles (waveriders), the drag loss effect is minimal for trajectories with relatively high launch energies to the least distant outer planets. Drag does increase the minimum launch energy required to reach a particular planet, but this is a small effect compared to the tremendous advantages of aerogravity assists.

Acknowledgment

Portions of the work described were performed at the Jet Propulsion Laboratory, California Institute of Technology, under contract with NASA.

References

[1]Nonweiler, T. R. F., "Aerodynamic Problems of Manned Space Vehicles," *Journal of the Royal Aeronautical Society*, Vol. 63, No. 585, 1959, pp. 521–528.

[2]Bowcutt, K. G., Anderson, J. D., and Capriotti, D. P., "Viscous Optimized Hypersonic Waveriders," AIAA Paper 87-0272, Jan. 1987.

[3]Lewis, M. J., and McRonald, A. D., "Design of Hypersonic Waveriders for Aeroassisted Interplanetary Trajectories," *Journal of Spacecraft and Rockets*, Vol. 29, No. 5, 1992, pp. 653–660.

[4]Anderson, J. D., Lewis, M. J., Kothari, A. P., and Corda, S., "Hypersonic Waveriders for Planetary Atmospheres," *Journal of Spacecraft and Rockets*, Vol. 28, No. 4, 1991, pp. 401–410.

[5]Anderson, J. L., "Back from the Future," *Aerospace America*, Vol. 31, No. 11, 1993, pp. 32–36.

[6]Bender, D. F., "Trajectories to the Outer Planets Using Aero-Gravity Assist Flybys of Venus and Mars," American Astronautical Society, Paper 91-419, Aug. 1991.

[7]McRonald, A. D., and Randolph, J. E., "Hypersonic Maneuvering for Augmenting Planetary Gravity Assist," *Journal of Spacecraft and Rockets*, Vol. 29, No. 2, 1992, pp. 216–222.

[8]Randolph, J. E., and McRonald, A. D., "Solar System 'Fast Mission' Trajectories Using Aerogravity Assist," *Journal of Spacecraft and Rockets*, Vol. 29, No. 2, 1992, pp. 223–232.

[9]Williams, S. N., "Automated Design of Multiple Encounter Gravity-Assist Trajectories," M.S. Thesis, School of Aeronautics and Astronautics, Purdue Univ., West Lafayette, IN, Aug. 1990.

[10]Patel, M. R., "Automated Design of Delta-V Gravity-Assist Trajectories for Solar System Exploration," M.S. Thesis, School of Aeronautics and Astronautics, Purdue Univ., West Lafayette, IN, Aug. 1993.

[11]Sims, J. A., Longuski, J. M., and Patel, M. R., "Aerogravity-Assist Trajectories to the Outer Planets," International Academy of Astronautics, Paper L-0405P, April 1994.

[12]Lewis, M. J., "The Use of Hypersonic Waveriders for Aero-Assisted Orbital Manoeuvring," *Journal of the British Interplanetary Society*, Vol. 46, No. 1, 1993, pp. 11–20.

[13]Lind, C. A., and Lewis, M. J., "High Lift-to-Drag Hypersonic Configurations for Rapid Trajectories to Mars," *Journal of Practical Applications in Space*, Vol. 2, No. 2, 1991, pp. 55–89.

C. A. Kluever
Associate Editor